On the Performance of Tantalum Pentoxide and Silicon Nitride Slot Waveguides for On-Chip Raman Spectroscopy

(Student paper)

Zuyang Liu [1,2], Haolan Zhao [1,2], Ali Raza [1,2], Nicolas Le Thomas [1,2], and Roel Baets [1,2]
[1]*Photonics Research Group, INTEC Department, Ghent University-imec, 9052 Ghent, Belgium*
[2]*Center for Nano- and Biophotonics, Ghent University, 9052 Ghent, Belgium*
e-mail: Zuyang.Liu@ugent.be

ABSTRACT

Waveguide-enhanced Raman spectroscopy is a promising technique for high-sensitivity molecular identification and quantification. Efficient on-chip Raman spectroscopy demands high-index-contrast waveguide platforms and a reduced photonic Raman background of the waveguide core material. Tantalum pentoxide is recently emerging as a novel CMOS compatible integrated platform. It has a moderately high refractive index of 2.11, along with a low Raman background. In this article, we investigate and identify the optimal waveguide geometry of tantalum pentoxide slot waveguides to reach the highest overall Raman collection efficiency and lowest waveguide background. Compared to the widely used silicon nitride waveguide platform, tantalum pentoxide waveguides delivers 4 times better performance concerning signal-to-noise ratio (SNR), assuming similar waveguide loss values.

Keywords: On-chip Raman spectroscopy, waveguide sensor, high-index-contrast platforms

1 INTRODUCTION

Raman spectroscopy is a label-free technique that probes the vibrational modes of molecules. These vibrational modes constitute the "fingerprints" of chemical bonds, which can be used for unambiguous molecular identification and quantification. A major challenge intrinsic to Raman spectroscopy is the extremely weak signal. One method to enhance the collection of the signal is to make use of a photonic waveguide [1]-[5]. In waveguide enhanced Raman spectroscopy, the evanescent tail of the waveguide mode overlaps with analytes, and it is employed to excite and collect the Raman signal. The tight confinement of the optical field not only enhances the light-matter interaction but also allows for an efficient collection of the generated signal. Silicon nitride waveguides have been widely explored for on-chip Raman spectroscopy of various analytes, including bulk liquids [1], monolayers [2], and low-concentration gases [4], [5]. However, PECVD silicon nitride optimized for Raman sensing has only a moderate refractive index of 1.89 and a relatively high Raman background, which induces limits in detection limit for analytes with a low concentration or a weak Raman scattering cross-section.

Tantalum pentoxide (Ta_2O_5) has recently been proposed as a novel CMOS-compatible integrated photonic platform that might substitute silicon nitride [6], [7]. Ta_2O_5 has a refractive index of 2.11 and a Raman background roughly three times lower than Si_3N_4 for vibrational modes above 1000 cm^{-1}, as shown in Figure 1(a) [8]. These advantages make Ta_2O_5 very interesting for on-chip Raman spectroscopic applications.

In this work, we compare the performance in terms of Raman collection of Ta_2O_5 and Si_3N_4 slot waveguides by taking into account the recently measured Raman background [8]. The impact of the waveguide geometry is presented systematically for both platforms.

2 METHOD OF SIMULATION

Assuming that the analyte molecules are uniformly distributed in the upper cladding with a molecular density ρ and differential Raman cross-section σ, the total power of backward-propagating Raman signal $P_s(\lambda)$ and Raman background P_{bg} normalized by the pump power are given by

$$\frac{P_s(\lambda)}{P_p} = \eta_0 \cdot \sigma(\lambda) \cdot \rho \cdot \frac{1-e^{-2\alpha L}}{2\alpha}, \qquad \frac{P_{bg}}{P_p} = \eta_{bg} \cdot \kappa \cdot \frac{1-e^{-2\alpha L}}{2\alpha}. \tag{1}$$

where α is the propagation loss, P_p is the pump power coupled into the waveguide, and L is waveguide length. κ is a phenomenological parameter that relates the strength of the Raman background to the thermodynamic fluctuations within the waveguide core [9]. It carries the same dimension as $\sigma \cdot \rho$. The specific conversion efficiencies for the signal and the background (η_0 and η_{bg}) with Stokes wavelength λ_S are defined as [1]

$$\eta_0 = \frac{n_g^2 \lambda_S^2 \iint_{\text{analyte}} |E(x,y)|^4 \mathrm{d}x\mathrm{d}y}{n_{\text{analyte}} \left(\iint_{\infty} \epsilon(x,y)|E(x,y)|^2 \mathrm{d}x\mathrm{d}y \right)^2}, \qquad \eta_{bg} = \frac{n_g^2 \lambda_S^2 \iint_{\text{waveguide core}} |E(x,y)|^4 \mathrm{d}x\mathrm{d}y}{n_{\text{core}} \left(\iint_{\infty} \epsilon(x,y)|E(x,y)|^2 \mathrm{d}x\mathrm{d}y \right)^2}. \tag{2}$$

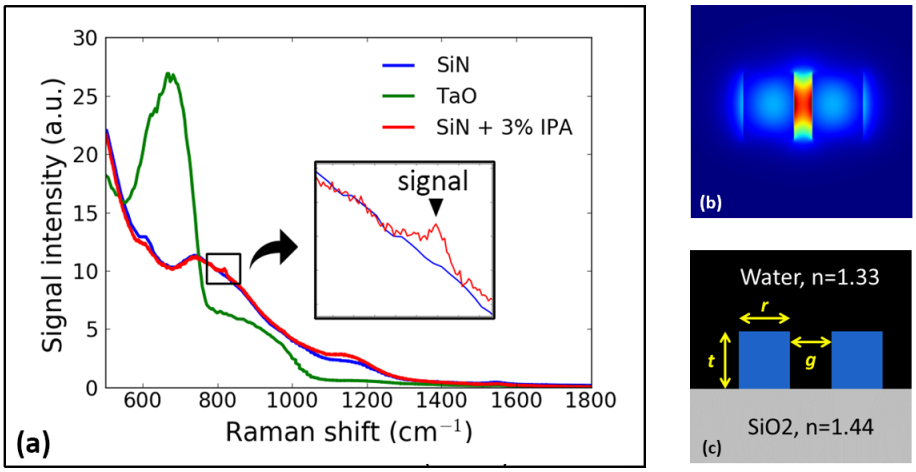

Figure 1. (a) The normalized Raman background of two platforms (reproduced from [8]) along with a typical spectrum obtained with low concentration (3%) of isopropyl alcohol (IPA) and a Si_3N_4 strip waveguide. Inset is a magnified view of the spectrum around the signal. In this situation, our ability to distinguish the signal is limited by the strength of the Raman background and the shot noise associated with it. (b) Typical electric field distribution on the slot waveguide. The field is strongly confined within the slot, inducing a much larger overlap with the analyte. (c) Waveguide cross-section with height t, gap width g and rail width r. The upper-cladding is assumed to be water, and the lower-cladding is assumed to be buried oxide. Waveguide core material are either Si_3N_4 and Ta_2O_5.

where the electric fields at pump and Stokes wavelengths are approximated to be identical. n_g is the group index of the mode, $E(x, y)$ is the electric field, and ϵ is the relative permittivity. η_0 and η_{bg} can be viewed as the product of the modal overlap factors at pump and Stokes wavelengths divided by the square of the modal area of the waveguide at these wavelengths.

For a given analyte and analyte density, we notice that the Raman signal and the background generated per unit length of a waveguide are determined uniquely by η_0 and η_{bg}. The signal-to-noise ratio (SNR) is proportional to the figure of merit (FOM) defined as

$$\mathrm{FOM} = \frac{\eta_0}{\sqrt{\eta_{bg}}}. \tag{3}$$

where we assume that the shot noise associated with Raman background is dominating the noise performance (as will be the case whenever the pump power is sufficiently high and the signal is weak relative to background).

Our analysis is limited to slot waveguides because they are known to perform better than strip or rib waveguides [10]. We compare the performance of Ta_2O_5 and Si_3N_4 slot waveguides through the numerically computed FOM. η_0 and η_{bg} are obtained from Lumerical MODE Solutions. In slot waveguides, the electric field of the TE mode is highly confined in the slot area (Figure 1(b)), resulting in stronger interaction with analytes. As illustrated in Figure 1(c), the under-cladding is assumed to be silicon dioxide (n=1.44) while the refractive index of the upper cladding is 1.33, representing water with a small analyte density. The waveguide geometry is determined uniquely by its height t, rail width r and gap g, with the gap always situated in the center of the waveguide. The FOM of both waveguide platforms with a thickness between 90 nm and 400 nm is shown in Figure 2. The rail width sweeps from 100 nm to 300 nm while the gap ranges from 20 nm to 80 nm.

3 RESULTS AND DISCUSSIONS

The performance of a series of Si_3N_4 and Ta_2O_5 slot waveguides are quantified at a pump wavelength of 785 nm using the aforementioned FOM. For each waveguide height, we analyzed the fundamental TE mode of various geometries on Si_3N_4 and Ta_2O_5 platforms separately. Results are shown in Figure 2. For Si_3N_4 slot waveguides, the optimal FOM improves with the increase of waveguide height, and its corresponding optimal geometry moves towards narrower gap and rail. The same tendency holds for Ta_2O_5 slot waveguides.

From the comparison between Si_3N_4 and Ta_2O_5 slot waveguides, we notice that almost every geometry exhibits better FOM on Ta_2O_5 platform, which agrees with our expectation. The optimal FOM of each height is indicated in Figure 2. Taking 300 nm height as an example, Ta_2O_5 can provide a FOM of 3.91, while the optimal FOM of Si_3N_4 is merely 1.60. Since the Raman background of Ta_2O_5 is roughly three times lower than Si_3N_4 for vibrational modes above 1000 cm^{-1} [8], we estimate that 300 nm Ta_2O_5 can provide 4.2 times higher SNR compared to Si_3N_4.

Apart from the shot noise generated by Raman background, the strength of the background itself also affects our ability to distinguish the signal because there is a practical limit in the accuracy of background subtraction..

Figure 1(c) displays a typical spectrum of waveguide-enhanced Raman spectroscopy with low concentration of analyte. The desired peak is almost buried by background features. In such a situation, it is convenient to consider another figure of merit namely signal-to-background ratio (SBR), which is proportional to η_0/η_{bg}. The computed SBR provided for a given geometry is always higher on the Ta_2O_5 platform. For 300 nm waveguide height, the Ta_2O_5 slot waveguide with optimal SNR generates 9.4 times higher SBR compared to the Si_3N_4 slot waveguide with optimal SNR.

It needs to be noted that the loss is not included in our simulations. If the propagation loss is not negligible, the SNR of waveguide geometries is related to the loss factor as

$$\mathrm{SNR} \propto \sqrt{\frac{1-e^{-2\alpha L}}{2\alpha}}, \tag{4}$$

resulting in a decrease of SNR with the increase of loss. Since narrower waveguides tend to have higher loss, the optimal geometry may change to a wider rail width.

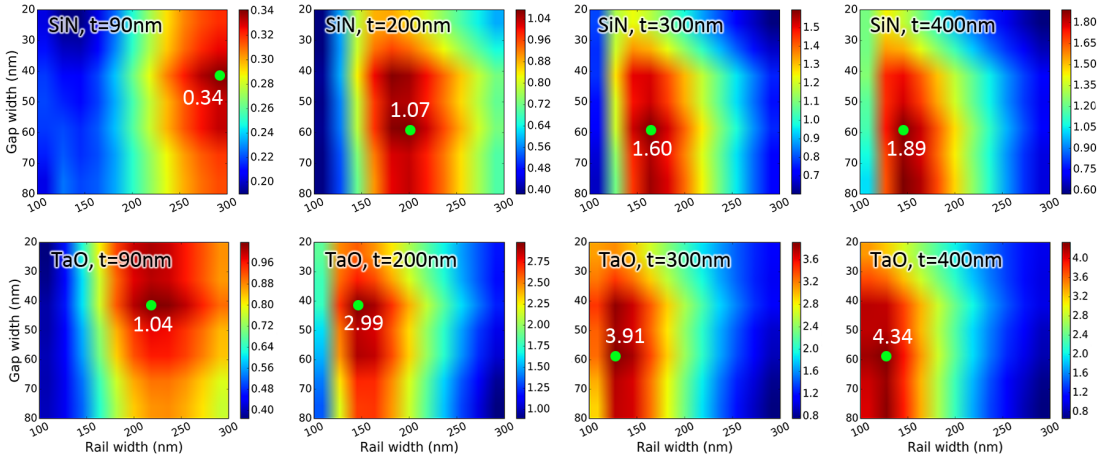

Figure 2. FOM of Si_3N_4 and Ta_2O_5 slot waveguide geometries obatined from numerical computation. The green circles indicate the optimal geometry and its corresponding FOM of each waveguide height.

4 CONCLUSIONS

We numerically computed the specific conversion efficiencies of Raman signal and background, and evaluated the performance of various slot waveguide geometries through calculation of SNR for two waveguide platforms. We conclude that Ta_2O_5 slot waveguides are considerably better than Si_3N_4 slot waveguides. When the height is 300 nm, Ta_2O_5 slot waveguides have a 4.2 times higher SNR and a 9.4 times higher SBR than Si_3N_4 waveguides.

REFERENCES

[1] A. Dhakal, A. Z. Subramanian, P. Wuytens, F. Peyskens, N. L. Thomas, and R. Baets, "Evanescent excitation and collection of spontaneous Raman spectra using silicon nitride nanophotonic waveguides," *Opt. Lett.*, vol. 39, no. 13, pp. 4025–4028, July 2014.

[2] A. Dhakal, P. C. Wuytens, F. Peyskens, K. Jans, N. L. Thomas, and R. Baets, "Nanophotonic Waveguide Enhanced Raman Spectroscopy of Biological Submonolayers," *ACS Photonics*, vol. 3, no. 11, pp. 2141–2149, Oct. 2016.

[3] C. Evans, C. Liu, and J. Suntivich, "TiO_2 Nanophotonic Sensors for Efficient Integrated Evanescent Raman Spectroscopy", *ACS Photonics*, vol. 3, no.9, pp. 1662–1669, July 2016.

[4] S. Holmstrom, T. Stievater, D. Kozak, M. Pruessner, N. Tyndall, W. Rabinovich, R. McGill, and J. Khurgin, "Trace gas Raman spectroscopy using functionalized waveguides," *Optica*, vol. 3, no. 8, pp. 891–896, Aug. 2016.

[5] N. Tyndall, T. Stievater, D. Kozak, K. Koo, R. McGill, M. Pruessner, W. Rabinovich, S. Holmstrom, "Waveguide-enhanced Raman spectroscopy of trace chemical warfare agent simulants," *Opt. Lett.*, vol. 43, no. 19, pp. 4803–4806, Oct. 2018.

[6] M. Belt, M. L. Davenport, J. E. Bowers, and D. J. Blumenthal, "Ultra-low-loss Ta_2O_5-core/SiO_2-clad planar waveguides on Si substrates," *Optica*, vol. 4, no. 5, pp. 532–536, May 2017.

[7] Z. Wang, M. N. Zervas, P. N. Bartlett, and J. S. Wilkinson, "Surface and waveguide collection of Raman emission in waveguide-enhanced Raman spectroscopy," *Opt. Lett.*, vol. 41, no. 17, pp. 4146–4149, Spet. 2016.

[8] A. Raza, S. Clemmen, M. de Goede, R. Ali, P. Hua, S. M. Garcia-Blanco, S. Honkanen, J. S. Wilkinson, and R. Baets, "High index contrast photonic platforms for on-chip Raman spectroscopy," in *Proc. ECIO 2018*, Valencia, Spain, May 2018, pp. 35–37.

[9] N. Le Thomas, A. Dhakal, A. Raza, F. Peyskens, and R. Baets, "Impact of fundamental thermodynamic fluctuations on light propagating in photonic waveguides made of amorphous materials," *Optica*, vol. 5, no.4, pp. 328–336, April 2018

[10] A. Dhakal, A. Raza, F. Peyskens, A. Z. Subramanian, S. Clemmen, N. Le Thomas, and R. Baets, "Efficiency of evanescent excitation and collection of spontaneous Raman scattering near high index contrast channel waveguides," *Opt. Express*, vol. 23, no. 21, pp. 27391–27404, Oct. 2015.